Heat Mass Transfer (2010) 46:881–890
DOI 10.1007/s00231-010-0637-z

ORIGINAL

Evaporative cooling and the Mpemba effect

M. Vynnycky · S. L. Mitchell

Received: 9 September 2009 / Accepted: 23 June 2010 / Published online: 8 July 2010

Abstract The Mpemba effect is popularly summarized by the statement that "hot water can freeze faster than cold", and has been observed experimentally since the time of Aristotle; however, there exist almost no theoretical models that predict the effect. With a view to initiating rigorous modelling activity on this topic, this paper analyzes in some depth the only available model in literature, which considers the potential role of evaporative cooling and treats the cooling water as a lumped mass. Certain omissions in the original work are highlighted and corrected, and results are obtained for a wide range of operating conditions—in particular, initial liquid temperature and cooling temperature. The implications and importance of the results of the model for experimental design are discussed, as are extensions of the model to handle more realistic 1-, 2- and 3-dimensional configurations.

List of symbols

A_0, A_1, A_2	Dimensionless constants
c_p	Specific heat capacity of water
C_p	Dimensionless specific heat capacity of water
$[c_p]$	Characteristic scale for c_p
k	Mass transfer proportionality constant
$\mathcal{L}$	Dimensionless constant $(L_e\ (T_0)/L_f)$
L_e	Latent heat of evaporation of water
$[L_e]$	Characteristic scale for L_e
L_f	Latent of freezing
m	Mass of water vapour
m_{liq}	Mass of water
$m_{\mathrm{liq},i}$	Initial mass of water
M	Mass of ice
p_a	Water vapour pressure of the surroundings
P_a	Dimensionless water vapour pressure of the surroundings
p_v	Water vapour pressure
P_v	Dimensionless water vapour pressure
$[p_v]$	Characteristic scale for p_v
Q_1, Q_2	Polynomials in $\exp(St\theta)$
St	Stefan number, $[c_p](T_m - T_0)/[L_e]$
t	Time
$[t]$	Characteristic time scale
t_f	Time taken for cooling sample to freeze
$t_{f,total}$	Total time taken for two cooling samples to freeze
t_0	Time taken for cooling sample to reach 0°C
$t_{0,total}$	Total time taken for two cooling samples to reach 0°C
T	Temperature
T_i	Initial water temperature
T_i^{crit}	Dimensional solutions to Eqs. (51) and (52)
T_m	Maximum water temperature (100°C)
T_0	Minimum water temperature (0°C)

Greek symbols

$\alpha_{\pm}$	Dimensionless constants
θ	Dimensionless temperature
θ_i	Dimensionless initial water temperature
$\theta_{i,f}^{crit}$	Solution to Eq. (52)
$\theta_{i,0}^{crit}$	Solution to Eq. (51)
Λ	Dimensionless latent heat of evaporation of water
μ	Dimensionless mass of water vapour
μ_{ice}	Dimensionless mass of ice
μ_{liq}	Dimensionless mass of water

M. Vynnycky (✉) · S. L. Mitchell
Mathematics Application Consortium for Science and Industry (MACSI), Department of Mathematics and Statistics, University of Limerick, Limerick, Republic of Ireland
e-mail: michael.vynnycky@ul.ie

$\mu_{\mathrm{liq},i}$	Dimensionless initial mass of water
ν	Dimensionless constant
τ	Dimensionless time ($t/[t]$)
τ_f	Dimensionless time taken for cooling sample to freeze
$\tau_{f,total}$	Total dimensionless time taken for two cooling samples to freeze
τ_0	Dimensionless time taken for cooling sample to reach 0°C
$\tau_{0,total}$	Total dimensionless time taken for two cooling samples to reach 0°C

1 Introduction

The observation that "hot water can freeze faster than cold" has been made on numerous occasions in history ever since the time of Aristotle [1]. It was rediscovered in the 20th century by a Tanzanian student, Erasto Mpemba; subsequently, it was reported by Mpemba and Osborne [2], and thereafter has been termed the Mpemba effect. At first sight, the phenomenon appears to be highly counterintuitive, and various hypotheses have been proposed in order to explain it. Amongst these are: evaporative cooling [3], the effect of dissolved gases [4], supercooling [5, 6] and natural convection [7, 8]. A recent review of the topic and its history are given by Jeng [9], who points out that many of the experiments that have been carried out to demonstrate the effect have been unsatisfactory in their conception, with insufficient care being taken regarding what is actually meant by the statement that "hot water can freeze faster than cold": whether it means the time taken for ice to appear, or rather the time taken for the entire cooling sample to freeze [5]. A further complicating feature is that the effect may have more than one cause, and that it may not occur at all under certain conditions.

The development of theoretical models to assist with the interpretation of experimental results is a potentially attractive, yet largely unexplored, activity in the context of the Mpemba effect. Of all the papers cited above, only the one by Kell [3] manages to provide any form of experimental and theoretical evidence simultaneously for the effect, whereas only Vynnycky and Kimura [8] consider a model, for the potential role of natural convection, that is up-to-date in terms of current knowledge of heat and mass transfer and numerical methods. Consequently, there is a need to develop systematically a suite of models that considers, one by one to begin with, possible mechanisms for the effect, in tandem with a possible experiment. In this context, the purpose of this paper is to consider the potential role of evaporative cooling as an explanation for the Mpemba effect. Although Kell's model for evaporative cooling [3] successfully predicts the Mpemba effect, and is qualitatively in line with his experimental results, it is perhaps surprising that the model is so successful: it does not explicitly take into account the actual geometry in which the experiment was carried out; it treats the cooling body of water and ice as a lumped mass and assumes it to be at a uniform temperature; and it completely neglects any conduction or convection that ought to be occurring in the cooling water. Furthermore, in our attempts to recalculate Kell's results, as a precursor to geometrically more realistic two- or three-dimensional models, we have found the model details to be incomplete: for example, the full model equations are not stated, some of the model parameters are not given, nor are the model's full implications for experimental design explored. Moreover, although Kell's model was published forty years ago, since when there has been significant progress in knowledge in heat and mass transfer, it is nevertheless important to examine its full implications before proceeding further with a more complete model: it remains the only model that demonstrates the effect, and the reason why it is successful may prove to be of relevance for understanding more detailed models that include, for example, convective and radiative heat loss from the surface of the fluid, natural convection, dissolved gases and so on.

The layout of our paper is as follows. In Sect. 2, we give a statement of the model assumptions and equations used by Kell [3], as well as filling in omitted details. In Sect. 3, we nondimensionalize the model equations and consider their properties analytically; the reason for doing this is to enable possible future generalization to other cooling and freezing liquids. In Sect. 4, we solve the equations numerically, in particular, we find parameter intervals, in terms of the initial water temperature and cooling temperature, for which the model predicts that the Mpemba effect will occur; our results are compared with those of Kell [3], and detailed consideration is given to how the model can be used in the design of experiments for systematically demonstrating the effect. Finally, in Sect. 5, we draw conclusions.

2 Model

Kell's model [3] for the cooling and subsequent freezing of a sample of water treats the water as a lumped mass, i.e. the water is assumed to be in a container with adiabatic walls and without a lid, and to be at a uniform temperature, T, that evolves with time, t. Cooling is assumed to occur by evaporation only; hence, convection in the water or supercooling are not considered. The rate of evaporation from the surface of the water is taken to be proportional to

the excess of the vapour pressure, p_v, of the liquid water over the partial pressure, p_a, of water vapour in the surrounding atmosphere. Thus, the rate of increase of mass of water vapour, m, is given by

$$\frac{dm}{dt} = k(p_v - p_a), \tag{1}$$

where k is a positive proportionality constant. Although Eq. (1) is rather simple in form, it does capture, either explicitly or implicitly, the parameters on which evaporation is thought to depend: amongst others, the water temperature, the ambient temperature, the air velocity, the relative humidity of the air and the area of the evaporating surface. In particular, p_v is a function of the water temperature, whereas p_a is a function of the ambient temperature; consequently, $p_v - p_a$ can be thought of as a measure of the relative humidity, in the sense that the evaporation rate increases as this quantity increases. The constant k, which was never explicitly given in Kell's paper, plays the role of a mass transfer coefficient and can be thought of as implicitly accounting for the air velocity and the area of the evaporating surface. Consequently, if these do not change during the course of an experiment, the assumption that k is constant might be reasonable, especially if the air velocity is controlled; the assumption that the area of the evaporating surface does not change seems more certain, especially for Kell's experiments with Dewar flasks. Note that dimensions of k are [L][T], indicating that surface area/air velocity could be a suitable combination.

An additional model equation comes from considering the global heat balance: setting the enthalpy loss of the liquid to be equal to the enthalpy required to vapourize the liquid gives

$$m_{\text{liq}} c_p dT = -L_e dm, \tag{2}$$

where m_{liq} is the mass of liquid water, c_p is the specific heat of liquid water and L_e is the latent heat of evaporation. Using (1), Eq. (2) can then be written more conveniently as an ordinary differential equation (ODE) in the form

$$\frac{dT}{dt} = -\frac{kL_e}{c_p m_{\text{liq}}}(p_v - p_a). \tag{3}$$

Note that p_v, c_p, L_e all depend on T, and can be found tabulated in literature [10, 11]; for the range of temperature that is of interest in this paper, i.e. between 0 and 100°C, the actual profiles turn out to be of critical importance, and we plot $p_v(T)$ and $L_e(T)$ in Fig. 1. We omit plotting $c_p(T)$ however, as this only changes by around 1% over this temperature interval.

In addition, although not explicitly stated by Kell [3], it is assumed that total mass is conserved, so that

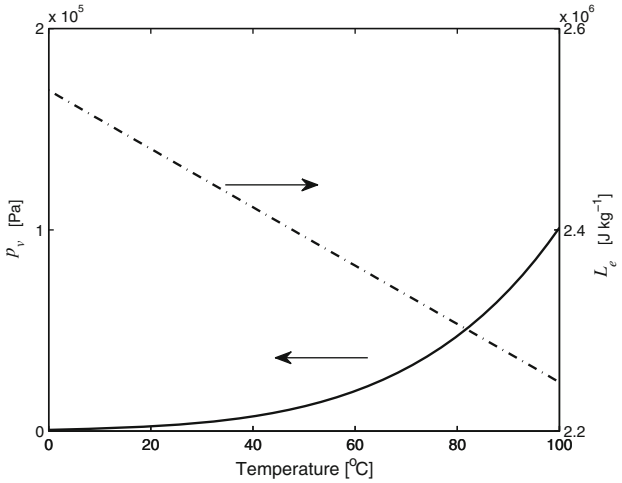

Fig. 1 p_v and L_e as functions of temperature between 0 and 100°C

$$\frac{d}{dt}\left(m_{\text{liq}} + m\right) = 0. \tag{4}$$

Observe also that the lumped mass assumption requires that there is a relation between the cooling surface and the volume of water; through Eqs. (1), (3) and (4), there is a relation between the surface conditions and the mass of the water and hence, by implication, the volume of the water. Subject to initial conditions that we shall discuss shortly, Eqs. (1), (3) and (4) constitute a plausible initial-value problem for T, m_{liq} and m, at least until T reaches 0°C, which we denote by T_0. However, once T reaches T_0, the model consists of Eq. (1), with p_v evaluated at this temperature, and a replacement for Eq. (2) that represents a balance of the enthalpy that is released by the freezing water and that released due to evaporation; this is expressed as

$$L_f dM = L_e dm, \tag{5}$$

where L_f is the latent heat of freezing and M is the mass of ice. Also, for this part of the process, we replace Eq. (4) by

$$\frac{d}{dt}\left(m_{\text{liq}} + m + M\right) = 0, \tag{6}$$

The model equations are then integrated until $m_{\text{liq}} = 0$, at which point complete freezing is deemed to have occurred.

Finally, the initial conditions are set to be

$$T(0) = T_i, \tag{7}$$

$$m(0) = 0, \tag{8}$$

$$m_{\text{liq}}(0) = m_{\text{liq},i}, \tag{9}$$

where T_i is the initial water temperature and $m_{\text{liq},i}$ is the initial mass of the water.

Two quantities that will be of particular interest are the time taken for the water to reach T_0, which we denote by t_0,

and the time taken for the water to freeze completely, which we denote by t_f; mathematically, these are defined by

$$t_0 := \{t | T(t) = T_0\}, \tag{10}$$

$$t_f := \{t | m_{\text{liq}}(t) = 0\}. \tag{11}$$

The main issue, namely the Mpemba effect, is then whether it is possible that there exist values of T_i, say $T_i = T_{i,1}, T_{i,2}$, such that if $T_{i,1} > T_{i,2}$, then $t_{0,1} < t_{0,2}$ and/or $t_{f,1} < t_{f,2}$, where $t_{0,j}$ and $t_{f,j}$ are the times taken to reach 0°C and for complete freezing, respectively, when starting at initial temperature $T_{i,j}$ ($j = 1,2$). In total, there can therefore be up to four cases to consider:

(I) no Mpemba effect;
(II) Mpemba effect with respect to t_0 only;
(III) Mpemba effect with respect to t_f only;
(IV) Mpemba effect with respect to both t_0 and t_f.

Although it is possible to solve equations (1), (3) and (4) subject to (7)–(9) numerically, a much greater understanding of the model comes from nondimensionalization and analysis, which we carry out next.

3 Analysis

3.1 Nondimensionalization

We nondimensionalize according to

$$\theta = \frac{T - T_0}{T_m - T_0}, \quad \mu = \frac{m}{m_{\text{liq},i}}, \quad \mu_{\text{liq}} = \frac{m_{\text{liq}}}{m_{\text{liq},i}}, \quad \mu_{\text{ice}} = \frac{M}{m_{\text{liq},i}}, \tag{12}$$

$$\tau = \frac{t}{[t]}, \quad C_p = \frac{c_p}{[c_p]}, \quad \Lambda = \frac{L_e}{[L_e]}, \quad P_v = \frac{p_v}{[p_v]}, \tag{13}$$

where $[t]$ is a suitable timescale that is yet to be determined, T_m is the maximum temperature of interest, i.e. the boiling point of water, and $[c_p]$, $[L_e]$ and $[p_v]$ are suitable scales for $c_p(T)$, $L_e(T)$ and $p_v(T)$, respectively, for $T_0 \le T \le T_m$; in view of Fig. 1, we take

$$[c_p] = c_p(T_0), \quad [L_e] = L_e(T_0), \quad [p_v] = p_v(T_m).$$

Then, (1) and (3) become

$$\frac{d\mu}{d\tau} = \left\{\frac{[t]k[p_v]}{m_{\text{liq},i}}\right\}(P_v(\theta) - P_a), \tag{14}$$

$$\frac{d\theta}{d\tau} = -\left\{\frac{[t]k[L_e][p_v]}{m_{\text{liq},i}[c_p](T_m - T_0)}\right\}\frac{\Lambda(\theta)(P_v(\theta) - P_a)}{(1-\mu)C_p(\theta)}, \tag{15}$$

respectively, where $P_a = p_a/[p_v]$. We could choose $[t]$ to be either

$$[t] = \frac{m_{\text{liq},i}[c_p](T_m - T_0)}{k[p_v][L_e]} \quad \text{or} \quad [t] = \frac{m_{\text{liq},i}[c_p](T_m - T_0)}{k[p_v]}, \tag{16}$$

and then there will be a dimensionless model parameter left in either (14) or (15) respectively. Without loss of generality, we set

$$[t] = \frac{m_{\text{liq},i}[c_p](T_m - T_0)}{k[p_v]}, \tag{17}$$

so that (14) and (15) now become

$$\frac{d\mu}{d\tau} = P_v(\theta) - P_a, \tag{18}$$

$$St\frac{d\theta}{d\tau} = -\frac{\Lambda(\theta)(P_v(\theta) - P_a)}{(1-\mu)C_p(\theta)}, \tag{19}$$

where St is the Stefan number, given by

$$St = \frac{[c_p](T_m - T_0)}{[L_e]}. \tag{20}$$

Also, we see that the values of $m_{\text{liq},i}$ and k are scaled out of the model equations. In practice, this means that, amongst other things:

- two samples having the same value of $m_{\text{liq},i}/k$ will show the same quantitative behaviour, e.g. they will freeze at exactly the same time;
- a sample having a greater value of $m_{\text{liq},i}/k$ than another sample will cool and freeze more slowly than the second sample, but both samples will exhibit the Mpemba effect for the same values of T_i.

In addition, Eqs. (18) and (19) are complemented by the nondimensional version of (4),

$$\frac{d}{d\tau}(\mu_{\text{liq}} + \mu) = 0, \tag{21}$$

whereas the initial conditions (7)–(9) are now

$$\theta(0) = \theta_i, \tag{22}$$

$$\mu(0) = 0, \tag{23}$$

$$\mu_{\text{liq}}(0) = 1, \tag{24}$$

with $\theta_i = (T_i - T_0)/(T_m - T_0)$. Finally, we have the dimensionless equivalents of (10) and (11) as

$$\tau_0 := \{\tau | \theta(\tau) = 0\}, \tag{25}$$

$$\tau_f := \{\tau | \mu_{\text{liq}}(t) = 0\}, \tag{26}$$

respectively. Also, for $\tau_0 < \tau \le \tau_f$, we have

$$\frac{d\mu}{d\tau} = P_v(0) - P_a, \tag{27}$$

Table 1 Parameter values

Parameter	Value	Units
$c_p(T_0)$	4217.4	J kg^{-1} K^{-1}
$L_e(T_0)$	2.54×10^6	J kg^{-1}
L_f	3.34×10^5	J kg^{-1}
$p_v(T_m)$	1.01×10^5	Pa
T_m	100	°C
T_0	0	°C

$$\frac{d}{d\tau}(\mu_{\text{ice}} - \mathcal{L}\mu) = 0, \tag{28}$$

$$\frac{d}{d\tau}(\mu_{\text{liq}} + \mu + \mu_{\text{ice}}) = 0, \tag{29}$$

where $\mathcal{L} = L_e(T_0)/L_f$. The starting conditions for (27)–(29) are

$$\mu(\tau_0) = \mu_0, \tag{30}$$

$$\mu_{\text{ice}}(\tau_0) = 0, \tag{31}$$

$$\mu_{\text{liq}}(\tau_0) = 1 - \mu_0. \tag{32}$$

In summary, we note that there are four model parameters: $\mathcal{L}$, P_a, St and θ_i. Using the data in Table 1, we have

$$\mathcal{L} \approx 7.6, \quad 0 \le P_a < P_v(0), \quad St \approx 0.17, \quad 0 \le \theta_i \le 1,$$

where $P_v(0) = 6.025 \times 10^{-3}$.

3.2 Analytical solutions

At this stage, analytic progress is possible if we take C_p as constant and Λ as a linear function of θ; this is motivated by the fact that $C_p(\theta) \approx 1$ and $\Lambda(\theta) = 1 - v\theta$ from Fig. 1 after nondimensionalization, where $v = 0.105$. Dividing (19) by (18), we obtain

$$\frac{St d\theta}{1 - v\theta} = -\frac{d\mu}{1 - \mu}, \tag{33}$$

which can be integrated, subject to (22) and (23), to obtain

$$\theta = \frac{1}{v}\left(1 - \frac{1 - v\theta_i}{(1-\mu)^{v/St}}\right). \tag{34}$$

Hence, when θ first reaches zero, i.e. when $\tau = \tau_0$, we will have

$$\mu_0 = 1 - (1 - v\theta_i)^{St/v}. \tag{35}$$

The governing equations for $\tau_0 < \tau \le \tau_f$, (27)–(29), can then be easily solved to give

$$\mu = \mu_0 + (P_v(0) - P_a)(\tau - \tau_0), \tag{36}$$

$$\mu_{\text{ice}} = \mathcal{L}(P_v(0) - P_a)(\tau - \tau_0), \tag{37}$$

$$\mu_{\text{liq}} = 1 - \mu_0 - (1 + \mathcal{L})(P_v(0) - P_a)(\tau - \tau_0), \tag{38}$$

which leads to

$$\tau_f = \tau_0 + \frac{1 - \mu_0}{(1 + \mathcal{L})(P_v(0) - P_a)}. \tag{39}$$

We return to the significance of this result later; for the time being we focus on determining τ_0.

Combining (19) and (34), we obtain

$$St\frac{d\theta}{d\tau} = -\frac{(1 - v\theta)^{1+St/v}(P_v(\theta) - P_a)}{(1 - v\theta_i)^{St/v}}, \tag{40}$$

leading to

$$\tau_0 = St(1 - v\theta_i)^{St/v} \int_0^{\theta_i} \frac{d\theta'}{(1 - v\theta')^{1+St/v}(P_v(\theta') - P_a)}. \tag{41}$$

Whilst it is possible to compute (41) by numerical quadrature, it would be convenient to have an expression in closed form to analyze in order to gain a better understanding of the model. A way to do this is to consider asymptotic solutions for $v \ll 1$; hence, we consider replacing (33) at leading order in v by

$$St d\theta = -\frac{d\mu}{1 - \mu}, \tag{42}$$

which can be solved to give

$$\theta = \theta_i + St^{-1}\ln(1 - \mu); \tag{43}$$

then, instead of (35), we now have

$$\mu_0 = 1 - \exp(-St\theta_i). \tag{44}$$

A comparison of (34) and (43) for θ as a function of μ for $\theta_i = 0.1$ and 1 is given in Fig. 2, and indicates that this approximation incurs little quantitative error for our value of $v = 0.105$ for a wide range of θ_i-values; this justifies the

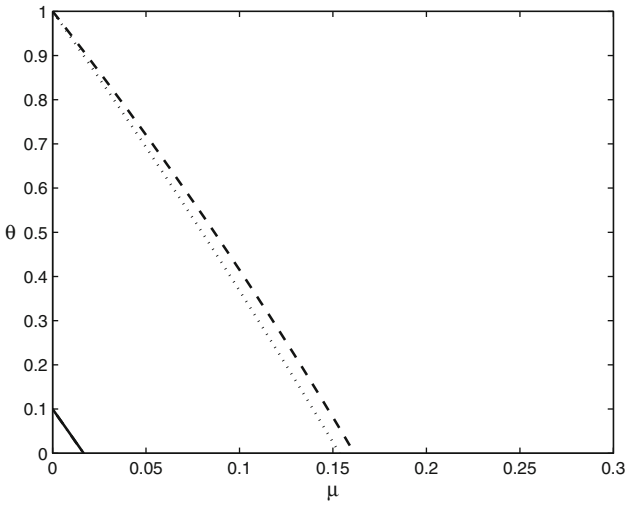

Fig. 2 θ as a function of μ for $\theta_i = 0.1$ and 1, as given by Eqs. (34) and (43): *continuous line* $\theta_i = 0.1$; *dashed dotted line* $\theta_i = 0.1 (v \ll 1)$; *dashed line* $\theta_i = 1$; *dotted line* $\theta_i = 1 (v \ll 1)$

simplification proposed. Note also from Fig. 2 that the two curves for $\theta_i = 0.1$ are literally on top of each other; thus, the approximation is better for lower values of θ_i.

Proceeding further, we have

$$St\frac{d\theta}{d\tau} = -\frac{(P_v(\theta) - P_a)}{\exp(St(\theta - \theta_i))}. \tag{45}$$

Now, whilst it would be possible to express $P_v(\theta)$ as a closed-form expression by integrating the Clausius–Clapeyron equation, it would however not be possible then to integrate (45) analytically; on the other hand, there would be some merit in being able to do so, in order to see which part of the model equations is indispensable for predicting the Mpemba effect. To this end, it proves instructive to replace P_v with forms which are qualitatively similar to it, but that do lead to analytical solutions to Eq. (45). We consider first

$$Q_1(\theta) := A_0 + A_1 \exp(St\theta), \tag{46}$$

where A_0 and A_1 are constants to be specified. We will set

$$Q_1(0) = P_v(0), \quad Q_1(1) = P_v(1),$$

which leads to

$$A_0 = \frac{P_v(0)\exp(St) - P_v(1)}{\exp(St) - 1}, \quad A_1 = \frac{P_v(1) - P_v(0)}{\exp(St) - 1}.$$

Replacing $P_v(\theta)$ by $Q_1(\theta)$ in Eq. (45) and setting $X = \exp(St\theta)$, we have

$$\frac{dX}{A_0 + A_1X - P_a} = -\exp(St\theta_i)d\tau, \tag{47}$$

which can be integrated to give

$$\ln\left(\frac{A_1\exp(St\theta_i) + A_0 - P_a}{A_1\exp(St\theta) + A_0 - P_a}\right) = A_1\exp(St\theta_i)\tau,$$

and hence

$$\tau_0 = A_1^{-1}\exp(-St\theta_i)\ln\left(\frac{A_1\exp(St\theta_i) + A_0 - P_a}{P_v(0) - P_a}\right). \tag{48}$$

Consider also

$$Q_2(\theta) := A_0 + A_1\exp(St\theta) + A_2\exp(2St\theta),$$

with now

$$Q_2(0) = P_v(0), \quad Q_2(1) = P_v(1),$$
$$Q_2'(0) = \frac{St(P_v(1) - P_v(0))}{2(\exp(St) - 1)},$$

i.e. the gradient of Q_2 at $\theta = 0$ is half that of Q_1. Then A_0, A_1 and A_2 are given by

$$A_0 = P_v(0) - \frac{(P_v(1) - P_v(0))(\exp(St) - 2)}{2(\exp(St) - 1)^2},$$

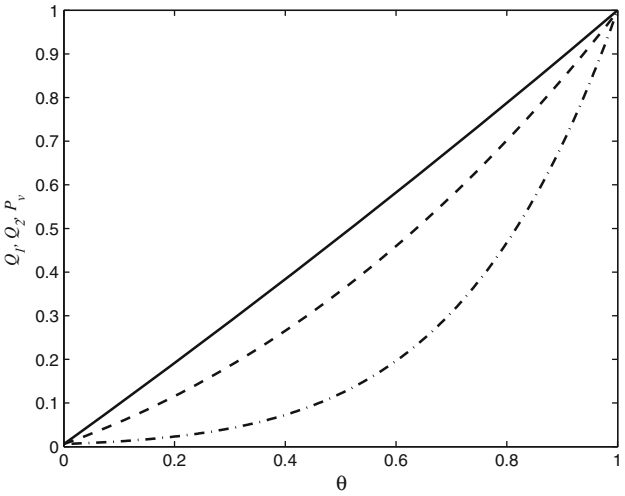

Fig. 3 Q_1 (*continuous line*), Q_2 (*dashed line*) and P_v (*dashed dotted line*) as functions of θ

$$A_1 = \frac{(P_v(1) - P_v(0))(\exp(St) - 3)}{2(\exp(St) - 1)^2},$$
$$A_2 = \frac{(P_v(1) - P_v(0))}{2(\exp(St) - 1)^2}.$$

A comparison of $P_v(\theta)$, $Q_1(\theta)$ and $Q_2(\theta)$ is given in Fig. 3. Observe that $Q_1(\theta)$ is almost linear whereas $Q_2(\theta)$ has a non-constant slope and is closer to $P_v(\theta)$. This time, instead of (47), we have

$$\frac{dX}{A_0 + A_1X + A_2X^2 - P_a} = -\exp(St\theta_i)d\tau, \tag{49}$$

leading eventually to

$$\ln\frac{(\exp(St\theta_i) + \alpha_+)(\exp(St\theta) - \alpha_-)}{(\exp(St\theta) + \alpha_+)(\exp(St\theta_i) - \alpha_-)} = -A_2(\alpha_+ + \alpha_-)\exp(St\theta_i)\tau,$$

where

$$\alpha_\pm = \sqrt{\frac{A_1^2}{4A_2^2} - \frac{(A_0 - P_a)}{A_2}} \pm \frac{A_1}{2A_2},$$

and hence,

$$\tau_0 = A_2^{-1}(\alpha_+ + \alpha_-)^{-1}\exp(-St\theta_i)\ln\frac{(1 + \alpha_+)(\exp(St\theta_i) - \alpha_-)}{(1 - \alpha_-)(\exp(St\theta_i) + \alpha_+)}. \tag{50}$$

In Fig. 4, we plot expressions (48) and (50) for τ_0 against θ_i and compare them against that obtained by numerical integration using the true expression for $P_v(\theta)$, namely that given in (41) above. Although perhaps difficult to discern from this plot, τ_0 does not attain a maximum for $Q_1(\theta)$, although it does do so for $Q_2(\theta)$ and $P_v(\theta)$, at $\theta_i = 0.82$ and

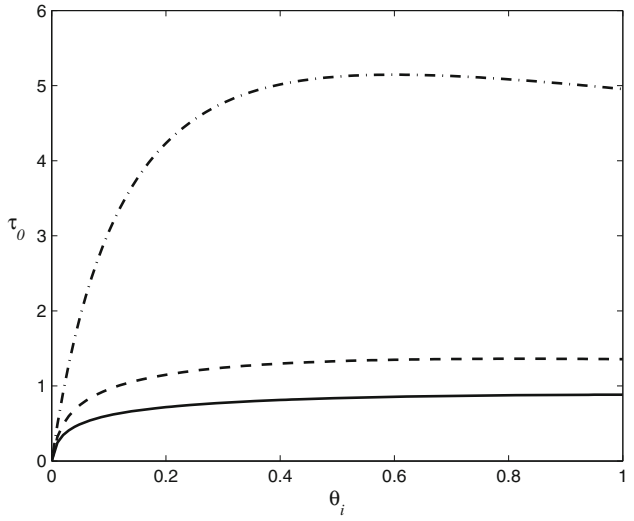

Fig. 4 τ_0 versus θ_i for Q_1 (*continuous line*), Q_2 (*dashed line*) and P_v (*dashed dotted line*); the Mpemba effect is seen for both the true water vapour pressure profile (P_v) and the qualitatively similar profile Q_2, but not for Q_1

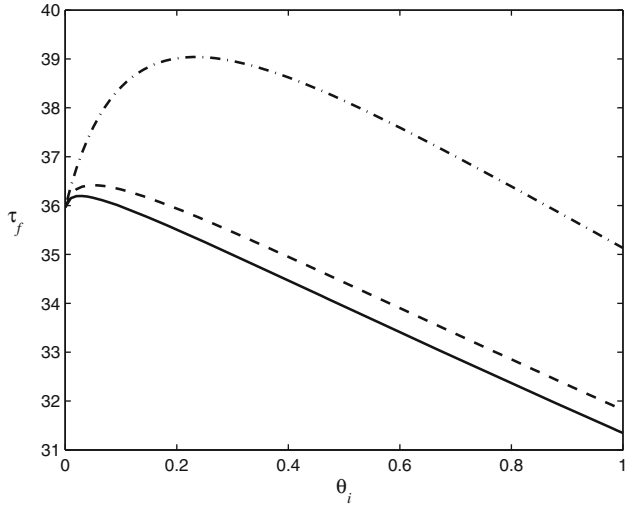

Fig. 5 τ_f versus θ_i for Q_1 (*continuous line*), Q_2 (*dashed line*) and P_v (*dashed dotted line*); the Mpemba effect is seen for all profiles, although the critical values of θ_i are different

0.6 respectively. On the other hand, a corresponding plot for τ_f, shown in Fig. 5, shows maxima for all profiles, i.e. Q_1, Q_2, P_v, although for different values of θ_i- 0.03, 0.05, 0.23, respectively. In general, Figs. 4 and 5 indicate that there is a link between the profile used for the vapour pressure and the time to taken to reach 0°C and to freeze completely: higher values of vapour pressure, i.e. in the sense that $Q_1(\theta) > Q_2(\theta) > P_v(\theta)$ for $0 < \theta < 1$, lead to shorter times.

Furthermore, Eq. (39), with μ_0 defined by (35), helps to explain the relation between these maxima. The maximum for τ_0 is given by the solution to

$$d\tau_0/d\theta_i = 0. \tag{51}$$

Using (39), the maximum for τ_f will be given by the solution to

$$\frac{d\tau_f}{d\theta_i} = \frac{d\tau_0}{d\theta_i} + \frac{St(1-v\theta_i)^{St/v-1}}{(1+\mathcal{L})(P_v(0)-P_a)} = 0. \tag{52}$$

Hence, because of the forms of the curves in Fig. 4, we can always expect that, if $0 < \theta_{i,f}^{crit}, \theta_{i,0}^{crit} < 1$, then

$$\theta_{i,f}^{crit} < \theta_{i,0}^{crit}, \tag{53}$$

where

$$\theta_{i,0}^{crit} := \{\theta_i |\, d\tau_0/d\theta_i = 0\}, \quad \theta_{i,f}^{crit} := \{\theta_i |\, d\tau_f/d\theta_i = 0\}.$$

Inequality (53) clearly holds for Q_2 and P_v, but there is no $\theta_{i,0}^{crit}$ such that $0 < \theta_{i,0}^{crit} < 1$ for Q_1. A related question is whether $0 < \theta_{i,f}^{crit} < 1$ for any form for $P_v(\theta)$. Differentiating Eq. (39) with respect to θ_i, after substitution of τ_0 from (41), we have

$$\left(\frac{d\tau_f}{d\theta_i}\right) = -St^2(1-v\theta_i)^{St/v-1}\int_0^{\theta_i}\frac{d\theta'}{(1-v\theta')^{1+St/v}(P_v(\theta')-P_a)} + \frac{St\left(1+\mathcal{L}-(1-v\theta_i)^{St/v}\right)}{(1+\mathcal{L})(1-v\theta_i)(P_v(\theta_i)-P_a)}, \tag{54}$$

and in particular

$$\left(\frac{d\tau_f}{d\theta_i}\right)_{\theta_i=0} = \frac{\mathcal{L}St}{(P_v(0)-P_a)(1+\mathcal{L})} > 0.$$

We see that the second term in (54) is always positive, whilst the first term is always negative; hence, if $\theta_{i,f}^{crit}$ does exist, it must be such that $\theta_{i,f}^{crit} > 0$, and occurs when the first term overtakes the second. Whether $\theta_{i,f}^{crit} < 1$ will depend on whether this happens quickly enough, which it does for all Q_1, Q_2 and P_v.

A further interesting observation here is that although previous authors have emphasized the role of mass loss in the Mpemba effect for the case of evaporative cooling [9], the results for τ_0 show that mass loss in itself is not sufficient: in addition, P_v must be of a form which leads to $\tau_0(\theta_i)$ having a maximum for $0 < \theta_i < 1$. Whilst water has a thermodynamically determined vapour pressure relation which clearly does give a maximum for $0 < \theta_i < 1$, this would not necessarily be the case for any other fluid for which one might perform such an experiment: for example, Mpemba's original observation was for an ice-cream mixture, rather than water, and another candidate which solidifies at a temperature that would be experimentally convenient is succinonitrile. On the other hand, mass loss is a necessary condition; without it, Eq. (45) becomes

$$St\frac{d\theta}{d\tau} = -(P_v(\theta) - P_a), \tag{55}$$

and it is evident that greater values of θ_i will lead to greater values of τ_0 since the right-hand side of Eq. (55) is strictly negative for $0 < \theta < 1$.

Having established the principal qualitative features of the model, we consider in greater detail numerical solutions for the model when $P_v(\theta)$ is used.

4 Results

All computations were done using the Matlab quadrature solve, quadl. For this, a continuous representation of the tabulated data from [10] for the nondimensional vapour pressure, $P_v(\theta)$, was required; this was done using cubic splines. In addition, we have implemented the correction suggested by Lange [10] for $P_v(0)$ when ice is in contact with both its own vapour and air, i.e. when $\tau_0 \leq \tau \leq \tau_f$.

Figure 6 shows the results of our re-computation of the cases considered in [3] for the relative time, τ_{rel}, to cooling and freezing; the forms of these curves are quantitatively similar to those in the original paper, and we therefore believe we have reproduced the original model correctly. In particular, curves *a*–*d* attain their maxima at $T_i = 66$, 32, 60 and 23°C, respectively. Moreover, Kell does not say what the times obtained are relative to, but it seems reasonable to assume, in view of his plot, that it is relative to the value of τ_f when $T_i = 0$°C and $p_a = 0$ Pa. Whilst one drawback of this particular model is that it cannot predict absolute times, the relative times that it can predict are in themselves useful: for example, curve *d* in Fig. 6 indicates that it would take roughly the same amount of time for a sample initially at 80°C to freeze completely as a sample initially at 10°C, when the cooling temperature for both is −10°C.

In addition, in Fig. 7, we plot m_{liq} as a function of T when $m_{\text{liq},i} = 1.55$ kg, $T_i = 88$°C and $p_a = 286.5$ Pa, which corresponds to the vapour pressure of water at −10°C, and compare this with Kell's theoretical and experimental results, which are for m_{liq} when $T = 39$°C; our theoretical value for m_{liq}, 1.429 kg, compares with his value of 1.43 kg, whereas the value obtained experimentally by Kell [3] was 1.44 kg.

Figure 8 shows how the locations of $T_{i,f}^{crit}$ and $T_{i,0}^{crit}$, which are defined, via Eq. (12), as the dimensional equivalents of $\theta_{i,f}^{crit}$ and $\theta_{i,0}^{crit}$ respectively, vary with p_a; thus, the Mpemba effect can be demonstrated provided the starting temperatures for both experiments lie above the curves. For values of T_i lying above the upper curve (IV), cooling to 0°C and complete freezing will occur more quickly for a higher value of T_i. For T_i between the two

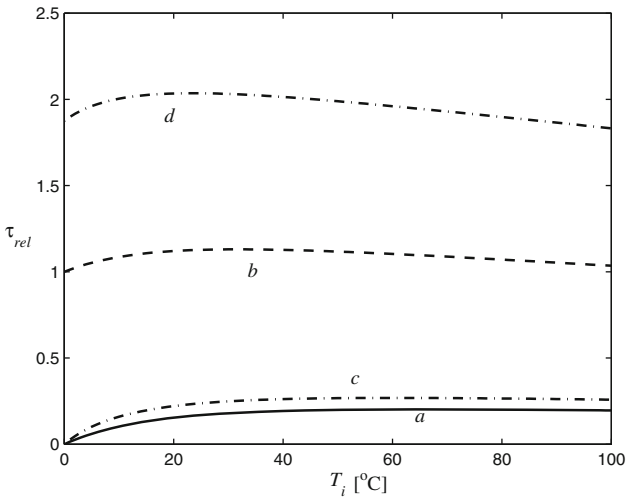

Fig. 6 Curves *a* and *c* give the relative time to cool to the freezing point, and *b* and *d* the time to finish freezing. For *a* and *b*, the partial pressure, p_a, is zero; for *c* and *d*, it corresponds to the vapour pressure of liquid water at −10°C. The results shown are for the same parameters as in Fig. 1 of [3] and indicate very good agreement

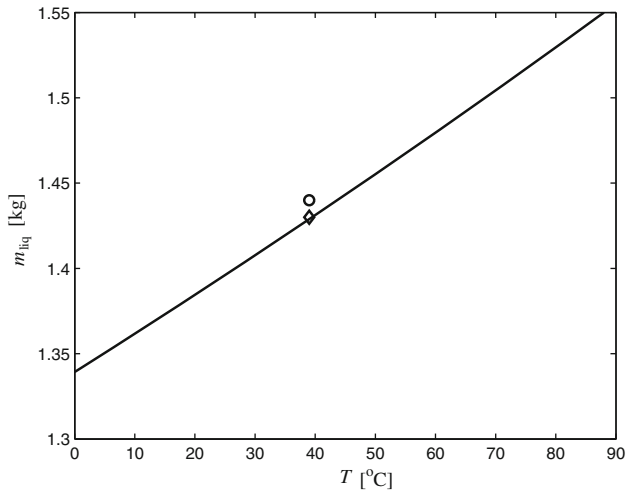

Fig. 7 m_{liq} versus T for $T_i = 88$°C and comparison with Kell's experimental (*open circle*) and model (*open diamond*) results

curves (III), cooling to 0°C will occur more slowly, but complete freezing faster, for a higher value of T_i. For T_i below the lower curve (I), the Mpemba effect would not be seen at all. Consequently, a region with property II, as defined in Sect. 2, does not appear at all.

However, Fig. 8 does not give a complete picture as regards all combinations of T_i that are possible; it only indicates the minimum value that one of the values of T_i must have in order for the effect to be seen. Denoting the initial water temperatures of two cooling and freezing experiments by $T_{i,1}$ and $T_{i,2}$, it is, for example, evident from Fig. 5 that it would be possible to demonstrate the effect by taking

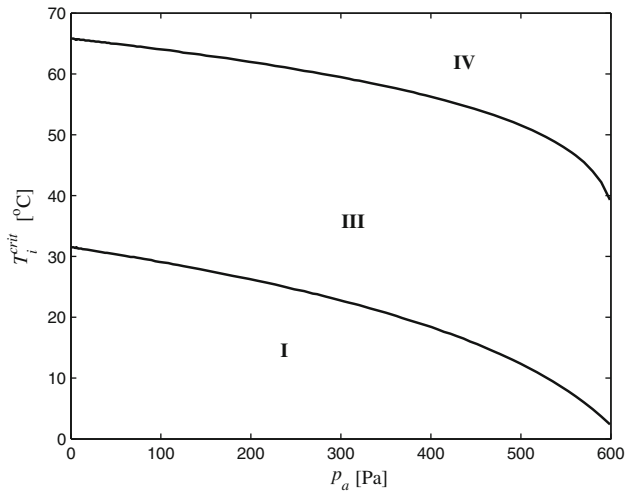

Fig. 8 T_i^{crit} as a function of p_a and the delineation of three possible regions: no Mpemba effect (I); Mpemba effect with respect to t_f only (III); Mpemba effect with respect to t_0 and t_f (IV)

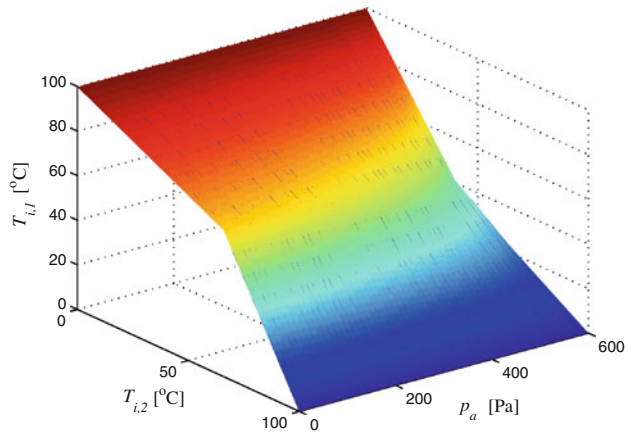

Fig. 9 All ($T_{i,1}$, $T_{i,2}$, p_a)-combinations above the surface lead to the Mpemba effect with respect to t_0. The surface is symmetric about $T_{i,1} = T_{i,2}$

$$T_{i,1} > T_{i,f}^{crit}, \quad T_{i,2} < T_{i,f}^{crit},$$

provided we also make sure that $T_{i,2} > T_f^*$, where

$$T_f^* := \left\{ T_{i,2} \middle| t_f(T_{i,2}) = t_f(T_{i,1}) \right\}.$$

Note also from Fig. 5 that if $T_{i,1}$ is large enough (around 0.83), then we simply have $T_f^* = 0$°C. Hence, a more complete picture of all possible experiments that would demonstrate the effect is given by plotting surfaces in ($T_{i,1}$, $T_{i,2}$, p_a)-space; as before, it is necessary to consider t_0 and t_f. Figure 9 shows the relevant plot for t_0, whilst Fig. 10 shows the corresponding plot for t_f; all ($T_{i,1}$, $T_{i,2}$, p_a)-combinations above each surface lead to the Mpemba effect with respect to t_0 and t_f, respectively. In both plots, the surface is symmetric about $T_{i,1} = T_{i,2}$, and the intersection of the surface with that plane in each plot

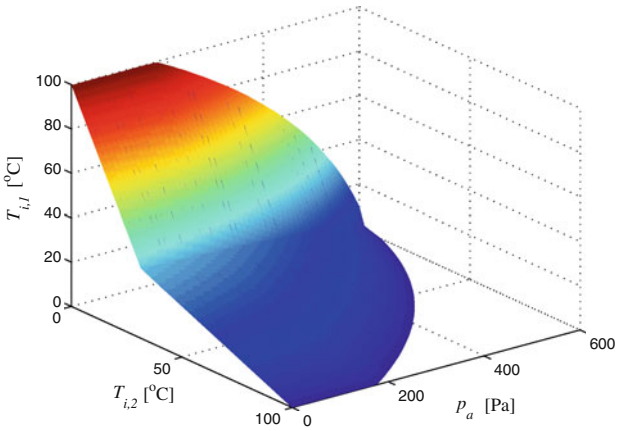

Fig. 10 All ($T_{i,1}$, $T_{i,2}$, p_a)-combinations above the surface lead to the Mpemba effect with respect to t_f. The surface is symmetric about $T_{i,1} = T_{i,2}$

corresponds to each of the curves given in Fig. 8. Furthermore, were we to superpose the surfaces shown in Figs. 8 and 9 onto a single plot, we would obtain three regions, corresponding to I, III and IV, as in Fig. 8.

Also of interest is how much total experimental time is necessary in order to demonstrate the effect, especially in view of potentially lengthy freezing times for water. Suppose we consider experiments that are intended to show the Mpemba effect with respect to time taken for the first appearance of ice, t_0, and that the experiments are carried out sequentially, first with $T_i = T_{i,1}$, then with $T_i = T_{i,2}$. To minimize the overall time $t_{0,total}$, it is clear that we should take $T_{i,1} > T_{i,2}$; the effect will then be shown after time $2t_{0,1}$, consisting of $t_{0,1}$ for the first experiment until complete freezing, and $t_{0,1}$ for the second experiment in order to confirm that complete freezing has not yet occurred. Consequently, the minimum total time for any ($T_{i,1}$, $T_{i,2}$)-pair can be expressed in terms of one quantity, i.e. $t_{0,1}$; hence, it is possible to draw a surface plot in ($t_{0,total}$, $T_{i,1}$, p_a)-space which takes into account all combinations. Similar considerations can also be used for determining the minimum overall time necessary to demonstrate the Mpemba effect with respect to complete freezing, $t_{f,total}$. Defining

$$\tau_{0,total} := \frac{t_{0,total}}{[t]}, \quad \tau_{f,total} := \frac{t_{f,total}}{[t]},$$

Figures 11 and 12 show, respectively, $\tau_{0,total}$ and $\tau_{f,total}$ as functions of $T_{i,1}$ and p_a. From these, it is evident that complete freezing takes considerably longer than cooling to 0°C, but also that freezing time decreases rapidly with p_a.

5 Conclusions

In this paper, we have revisited an early, but still the only, model [3] for evaporative cooling as an explanation for the

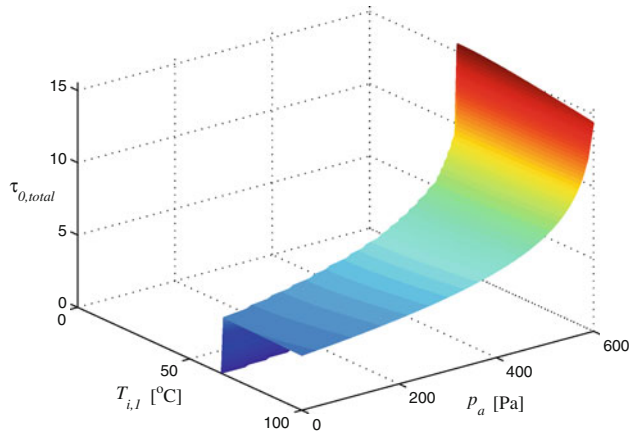

Fig. 11 Minimal total time necessary to see Mpemba effect with respect to the first appearance of ice

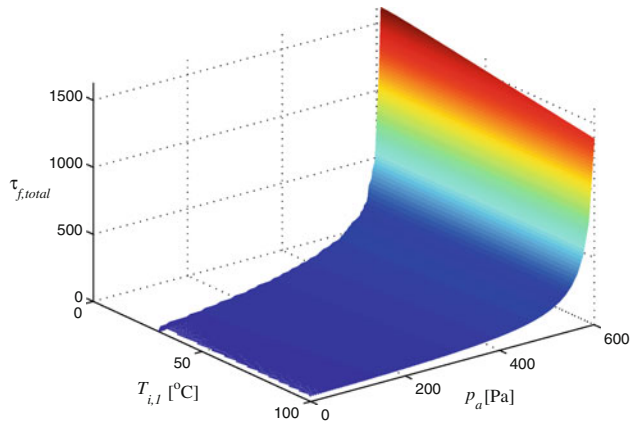

Fig. 12 Minimal total time necessary to see Mpemba effect with respect to complete freezing

Mpemba effect. Unlike the earlier paper, however, we have conducted a thorough analysis of the model and have also coupled its results to the important issue of experimental design, in particular with regard to:

- the experimental operating parameters that need to be employed in order to demonstrate the effect;
- which combinations of such parameters lead to the shortest experimental times.

In addition, our work has set the modelling of this phenomenon on a much firmer theoretical footing than the earlier work, and demonstrated the need for rigorous analysis in tandem with experiments, since the experimental reproduction of the phenomenon has proved elusive in the past.

In the context of the freezing of water, it is evident that mass loss to vapour of the initial sample and the water vapour pressure's (p_v) quantitative dependence on temperature play decisive roles; water's other temperature-dependent properties, such as latent heat of evaporation (L_e) and specific heat capacity (c_p) do not vary dramatically enough between 0 and 100°C to have much of an impact. The model also highlights other complications with regard to experimental observation: the Mpemba effect might occur with respect to the complete solidification of the sample, but not with respect to the first appearance of ice; however, the converse was not observed.

An important point to note is that the model shows quantitatively that, under appropriate conditions, evaporative cooling alone can cause the Mpemba effect. This observation serves as the basis for future 1D, 2D and 3D models; in such models, if scale analysis can be used to establish that cooling by evaporation is the dominant heat transfer mechanism, then there is a greater likelihood that such a model will also predict the occurrence of the Mpemba effect. In turn, this can be of use in helping with experimental design, with respect to geometry and cooling conditions; a particular example of this is the evaporative cooling of micron-sized droplets in a low-pressure aerosol reactor [12].

Acknowledgments The authors acknowledge the support of the Mathematics Applications Consortium for Science and Industry (www.macsi.ul.ie) funded by the Science Foundation Ireland Mathematics Initiative Grant 06/MI/005.

References

1. Walker J (2007) The flying circus of physics, 2nd edn. Wiley, Hoboken
2. Mpemba EP, Osborne DG (1969) Cool? Phys Educ 4:172–175
3. Kell GS (1969) The freezing of hot and cold water. Am J Phys 37:564–565
4. Wojciechowski B, Owczarek I, Bednarz G (1988) Freezing of aqueous solutions containing gases. Cryst Res Technol 23:843–848
5. Auerbach D (1995) Supercooling and the Mpemba effect. Am J Phys 63:882–885
6. Esposito S, De Risi L, Somma L (2008) Mpemba effect and phase transitions in the adiabatic cooling of water before freezing. Physica A 387:757–763
7. Maciejewski PK (1995) Evidence of a convective instability allowing warm water to freeze in less time than cold water. J Heat Transf 118:65–72
8. Vynnycky M, Kimura S (2008) Towards a natural-convection model for the Mpemba effect. In: 19th International symposium on transport phenomena, Reykjavik, Iceland. Paper 216 (CD-ROM), 17–20 August 2008
9. Jeng M (2006) The Mpemba effect: when can hot water freeze faster than cold? Am J Phys 74:514–522
10. Lange N (1946) Lange's handbook of chemistry, 6th edn. Handbook Publishers, Sandusky, Ohio
11. Cork JM (2007) Heat, 2nd edn. Wiley, New York
12. Fisenko SP, Wang W-N, Lenggoro IW, Okyuama K (2006) Evaporative cooling of micron-sized droplets in a low-pressure aerosol reactor. Chem Eng Sci 61:6029–6034